

# Extension of SBL Algorithms for the Recovery of Block Sparse Signals with Intra-Block Correlation

Zhilin Zhang, *Student Member, IEEE* and Bhaskar D. Rao, *Fellow, IEEE*

## Abstract

We examine the recovery of block sparse signals and extend the framework in two important directions; one by exploiting intra-block correlation and the other by generalizing the block structure. We propose two families of algorithms based on the framework of block sparse Bayesian learning (bSBL). One family, directly derived from the bSBL framework, requires knowledge of the block partition. Another family, derived from an expanded bSBL framework, is based on a weaker assumption about the a priori information of the block structure, and can be used in the cases when block partition, block size, block-sparsity are all unknown. Using these algorithms we show that exploiting intra-block correlation is very helpful to improve recovery performance. These algorithms also shed light on how to modify existing algorithms or design new ones to exploit such correlation for improved performance.

## Index Terms

Sparse Signal Recovery, Compressed Sensing, Block Sparsity, Cluster Structure, Sparse Bayesian Learning

## I. INTRODUCTION

Compressed sensing and the associated problem of sparse signal recovery have received much attention in recent years. The problem of sparse signal recovery is concerned with the recovery of a sparse signal

Z.Zhang and B.D.Rao are with the Department of Electrical and Computer Engineering, University of California at San Diego, La Jolla, CA 92093-0407, USA. Email:{z4zhang,brao}@ucsd.edu. The work was supported by NSF grant CCF-0830612. Parts of this work has been accepted to IEEE International Conference on Acoustics, Speech, and Signal Processing, 2012.

from a small number of its linear measurements. By sparse, we mean that only  $K$  elements of the signal are nonzero, where  $K$  is much less than the signal dimension. The model is given by

$$\mathbf{y} = \Phi \mathbf{x} + \mathbf{v}, \quad (1)$$

where,  $\mathbf{y} \in \mathbb{R}^{M \times 1}$  is the measurement vector.  $\Phi \in \mathbb{R}^{M \times N}$  ( $M \ll N$ ) is a known matrix.  $\mathbf{x} \in \mathbb{R}^{N \times 1}$  is the sparse signal which we want to recover and  $\mathbf{v}$  is the measurement noise vector. In some applications, the elements of  $\mathbf{x}$  have additional structure in addition to the sparsity property. A widely studied structure is the cluster/block structure [1]–[3]. A sparse signal with this structure can be viewed as a concatenation of  $g$  blocks, i.e

$$\mathbf{x} = [\underbrace{x_1, \dots, x_{d_1}}_{\mathbf{x}_1^T}, \dots, \underbrace{x_{d_{g-1}+1}, \dots, x_{d_g}}_{\mathbf{x}_g^T}]^T \quad (2)$$

where  $d_i, i = 1, \dots, g$ , are not necessarily the same. Among the  $g$  blocks, only  $k$  blocks are nonzero, where  $k \ll g$ . It is known that exploiting such block structure can further improve recovery performance [2], [3].

A number of algorithms have been proposed to recover such block sparse signals. These algorithms can be roughly classified into three categories. The first category, also the largest category, requires knowledge of the block partition, and may further need extra information such as the sparsity level (i.e. the total number of nonzero elements or nonzero blocks in  $\mathbf{x}$ ). Typical algorithms include Group Lasso [1], Group Basis Pursuit [4], Mixed  $\ell_2/\ell_1$  Program [5], and Block-OMP [3]. The second category does not need to know the block partition, but needs to know other a priori information, such as the sparsity level, or the potential block sizes. This category includes StructOMP [6], Block-CoSaMp [2] and some variants of Block-OMP. The last category requires very little a priori knowledge, and includes algorithms such as CluSS-MCMC [7] and BM-MAP-OMP [8].

However, to the best of our knowledge, none of the existing algorithms consider intra-block correlation, i.e. correlation among elements within each block. In practical applications such intra-block correlation is widely present. For example, in the compressed sensing of an image [6], [8], each block corresponds to a patch in the image, while in each individual patch, pixels have very similar tone indicating their amplitudes are highly correlated (if the image is modeled as a random field).

In this paper we derive several algorithms that adaptively learn and exploit the intra-block correlation for better performance. These algorithms are based on our recently proposed block sparse Bayesian learning (bSBL) framework [9]. Although the bSBL framework has been used to derive algorithms for other related models, this framework has not yet to be used in the block sparse model (1)-(2). The success

of SBL based methods in past contexts motivates us to consider their extension to this problem and fill this gap.

First, we derive two algorithms directly from the bSBL framework. Then we exploit the connection of the bSBL framework, which minimizes cost functions of hyper-parameters, to the standard framework used in most existing algorithms, which optimizes cost functions of  $\mathbf{x}$ . A novel hybrid algorithm is obtained. It not only has the ability of the two proposed bSBL algorithms, namely the ability to adaptively learn and exploit the intra-block correlation, but also has the speed advantage of group-Lasso type algorithms. The three proposed algorithms require a priori knowledge on the block partition. To overcome this limitation we next extend them to deal with problems when the block partition is unknown.

One contribution of our work is that our proposed algorithms are the first ones in the category that *adaptively* learn and exploit the intra-block correlation for improved performance. Extensive experiments have been conducted and they show that our proposed algorithms significantly outperform competitive algorithms especially when such correlation is high. We also propose a promising strategy to compensate the shortcoming of most existing algorithms that cannot adaptively exploit intra-block correlation.

Another contribution is the insight into the impact of correlation on performance. It is generally viewed that the multiple measurement vector model (MMV) [10] is a special case of the block sparse model [5]. But we find the impact of intra-block correlation in the block sparse model based algorithms is quite different to the impact of temporal correlation [9] in the MMV model based algorithms. Particularly, unlike the MMV case, if an algorithm ignores the intra-block correlation, whether such correlation is high or low, its recovery performance is about the same. However, if an algorithm exploits such correlation, it can greatly improve its recovery performance.

The third contribution is the development of a simple approximate model and corresponding algorithms to solve the problem when the block partition is entirely unknown. Extensive experiments find this approximate model and corresponding algorithms to be very effective especially in noisy environments.

We introduce the notations used in this paper. Bold symbols are reserved for vectors and matrices. Particularly,  $\mathbf{I}_d$  denotes the identity matrix with size  $d \times d$ . When the dimension is evident from the context, for simplicity, we just use  $\mathbf{I}$ .  $\text{diag}\{a_1, \dots, a_g\}$  denotes a diagonal matrix with principal diagonal elements being  $a_1, \dots, a_g$  in turn; if  $\mathbf{A}_1, \dots, \mathbf{A}_g$  are square matrices, then  $\text{diag}\{\mathbf{A}_1, \dots, \mathbf{A}_g\}$  denotes a block diagonal matrix with principal diagonal blocks being  $\mathbf{A}_1, \dots, \mathbf{A}_g$  in turn.  $\text{Tr}(\mathbf{A})$  denotes the trace of  $\mathbf{A}$ .  $\gamma \succeq \mathbf{0}$  means each element in  $\gamma$  is nonnegative.

## II. OVERVIEW OF THE BSBL FRAMEWORK

In this section we briefly describe the block sparse Bayesian learning framework [9], which is the basis of the algorithm development. In this framework, each block  $\mathbf{x}_i \in \mathbb{R}^{d_i \times 1}$  is modeled as a parameterized multivariate Gaussian distribution:

$$p(\mathbf{x}_i) \sim \mathcal{N}(\mathbf{0}, \gamma_i \mathbf{B}_i) \quad i = 1, \dots, g$$

Here  $\gamma_i$  is a nonnegative parameter controlling the block-sparsity of  $\mathbf{x}$ . When  $\gamma_i = 0$ , the  $i$ -th block becomes zero. During the learning procedure most  $\gamma_i$  tend to be zero, due to the mechanism of automatic relevance determination (ARD) [11], [12]. Thus sparsity in the block level is encouraged.  $\mathbf{B}_i \in \mathbb{R}^{d_i \times d_i}$  is a positive definite matrix, capturing the correlation structure of the  $i$ -th block. The prior of  $\mathbf{x}$  is  $p(\mathbf{x}) \sim \mathcal{N}(\mathbf{0}, \mathbf{\Sigma}_0)$ , where  $\mathbf{\Sigma}_0$  is a block-diagonal matrix with each principal block given by  $\gamma_i \mathbf{B}_i$ . Assume the noise vector satisfies  $p(\mathbf{v}) \sim \mathcal{N}(\mathbf{0}, \lambda \mathbf{I})$ , where  $\lambda$  is a positive scalar. Therefore the posterior of  $\mathbf{x}$  is given by  $p(\mathbf{x}|\mathbf{y}; \lambda, \{\gamma_i, \mathbf{B}_i\}_{i=1}^g) = \mathcal{N}(\boldsymbol{\mu}_x, \mathbf{\Sigma}_x)$  with

$$\boldsymbol{\mu}_x = \mathbf{\Sigma}_0 \boldsymbol{\Phi}^T (\lambda \mathbf{I} + \boldsymbol{\Phi} \mathbf{\Sigma}_0 \boldsymbol{\Phi}^T)^{-1} \mathbf{y} \quad (3)$$

$$\mathbf{\Sigma}_x = (\mathbf{\Sigma}_0^{-1} + \frac{1}{\lambda} \boldsymbol{\Phi}^T \boldsymbol{\Phi})^{-1} \quad (4)$$

Once the hyperparameters  $\lambda, \{\gamma_i, \mathbf{B}_i\}_{i=1}^g$  are estimated, the Maximum-A-Posterior (MAP) estimate of  $\mathbf{x}$  can be directly obtained from the mean of the posterior. The hyperparameters are generally estimated by a Type II maximum likelihood procedure [13], i.e. maximizing the likelihood of the hyperparameters where  $\mathbf{x}$  is integrated out. This is equivalent to minimize the negative log-likelihood

$$\begin{aligned} \mathcal{L}(\Theta) &\triangleq -2 \log \int p(\mathbf{y}|\mathbf{x}; \lambda) p(\mathbf{x}; \{\gamma_i, \mathbf{B}_i\}_{i=1}^g) d\mathbf{x} \\ &= \log |\lambda \mathbf{I} + \boldsymbol{\Phi} \mathbf{\Sigma}_0 \boldsymbol{\Phi}^T| + \mathbf{y}^T (\lambda \mathbf{I} + \boldsymbol{\Phi} \mathbf{\Sigma}_0 \boldsymbol{\Phi}^T)^{-1} \mathbf{y}, \end{aligned} \quad (5)$$

where  $\Theta$  denotes all the hyperparameters  $\lambda, \{\gamma_i, \mathbf{B}_i\}_{i=1}^g$ . Similar to the proof of the Theorem 1 in [9], we can show in the noiseless cases, when the number of nonzero entries in  $\mathbf{x}$  is less than  $M/2$ , the global minimum of the cost function (5) corresponds to the true solution (i.e. the sparsest solution), irrespective of the values of  $\mathbf{B}_i$ . This framework is called the block sparse Bayesian learning (bSBL) framework [9], an extension of the basic SBL framework [12].

Each algorithm derived from this framework includes three types of learning rules, namely, the learning rules for  $\gamma_i$ ,  $\mathbf{B}_i$ , and  $\lambda$ . The learning rule for  $\gamma_i$  is the main body of an algorithm. Different  $\gamma_i$  learning rules lead to different speed <sup>1</sup>, and determine the possible best recovery performance if one is given

<sup>1</sup>The  $\lambda$  learning rule also affects the speed, but its effect is not dominant.

optimal values of  $\lambda$  and  $\mathbf{B}_i$  [14]. The  $\lambda$  learning rule is also important. If one is unable to find an optimal (or a good suboptimal) value for  $\lambda$ , the recovery performance can be very poor even if the  $\gamma_i$  learning rule could potentially lead to perfect recovery performance. Thus, the match of a  $\lambda$  learning rule and a  $\gamma_i$  learning rule is crucial to an algorithms' performance. As for  $\mathbf{B}_i$ , it can be shown that its value does not affect the global minimum of the bSBL cost function (5), but only affect local minima and the domain of attraction of the global minimum [9]. So, one can impose various constraints on the forms of  $\mathbf{B}_i$  to achieve better performance and also prevent overfitting.

### III. ALGORITHMS FOR KNOWN BLOCK PARTITION

In this section we propose three algorithms, which require knowledge of the block partition. The first two are directly derived from the bSBL cost function (5). The third is obtained by drawing the connection of the bSBL cost function to the popular cost functions used by many algorithms such as Group Lasso and Mixed  $\ell_2/\ell_1$  Program. Some insights are gained from this connection and a promising strategy to improve existing algorithms is proposed.

#### A. BSBL-EM: the EM method

This algorithm can be readily derived from our previous work [9] on the MMV model with suitable adaptation. So we omit the derivation and only present the algorithm. However, several necessary changes, particularly for enhancing the robustness of the learning rules for  $\lambda$  and  $\mathbf{B}_i$  have to be made for the block sparsity model considered in this work.

Using the EM method [9], we can derive the learning rules for  $\gamma_i$  and  $\lambda$ :

$$\gamma_i \leftarrow \frac{1}{d_i} \text{Tr}[\mathbf{B}_i^{-1}(\boldsymbol{\Sigma}_x^i + \boldsymbol{\mu}_x^i(\boldsymbol{\mu}_x^i)^T)], \quad \forall i \quad (6)$$

$$\lambda \leftarrow \frac{\|\mathbf{y} - \Phi \boldsymbol{\mu}_x\|_2^2 + \text{Tr}(\boldsymbol{\Sigma}_x \Phi^T \Phi)}{M}. \quad (7)$$

where  $\boldsymbol{\mu}_x^i$  is the corresponding  $i$ -th block in  $\boldsymbol{\mu}_x$  (with the size  $d_i \times 1$ ), and  $\boldsymbol{\Sigma}_x^i$  is the corresponding  $i$ -th principal diagonal block in  $\boldsymbol{\Sigma}_x$  (with the size  $d_i \times d_i$ ).

The  $\lambda$  learning rule (7), as in existing SBL algorithms, is not robust in low SNR cases. By numerical study, we empirically find that one of the reasons is the disturbance caused by the off-block-diagonal elements in  $\boldsymbol{\Sigma}_x$  and  $\Phi^T \Phi$ . So we set their off-block-diagonal elements to zero, leading to the learning rule:

$$\lambda \leftarrow \frac{\|\mathbf{y} - \Phi \boldsymbol{\mu}_x\|_2^2 + \sum_{i=1}^g \text{Tr}(\boldsymbol{\Sigma}_x^i (\Phi^i)^T \Phi^i)}{M}, \quad (8)$$

where  $\Phi^i \in \mathbb{R}^{M \times d_i}$  is the submatrix of  $\Phi$ , which correspond to the  $i$ -th block of  $\mathbf{x}$ . This  $\lambda$  learning rule is better than (7) in generally noisy environments (e.g. SNR < 20dB). In noiseless cases there is no need to use any  $\lambda$  learning rules. Just fixing  $\lambda$  to a very small value, e.g.  $10^{-10} \sim 10^{-15}$ , can lead to optimal performance. In our experiments we set  $\lambda = 10^{-14}$  for noiseless cases.

Similar to [9], using the EM method we can derive a learning rule for each  $\mathbf{B}_i$ . However, we observe that assigning each block with a different  $\mathbf{B}_i$  can result in overfitting. When blocks have the same size, an effective strategy to avoid overfitting is parameter averaging [9], i.e. constraining  $\mathbf{B}_i = \mathbf{B}, \forall i$ . Using this constraint, the learning rule for  $\mathbf{B}$  can be derived as follows:

$$\mathbf{B} \leftarrow \frac{1}{g} \sum_{i=1}^g \frac{\Sigma_x^i + \mu_x^i (\mu_x^i)^T}{\gamma_i}. \quad (9)$$

However, the algorithm's performance can be improved by further constraining the matrix  $\mathbf{B}$ . The idea is to find a positive definite and symmetric matrix  $\hat{\mathbf{B}}$  such that  $\hat{\mathbf{B}}$  is close to  $\mathbf{B}$  especially along the main diagonal and the main sub-diagonal. Based on this idea, a possible form of  $\hat{\mathbf{B}}$  is given by

$$\begin{aligned} \hat{\mathbf{B}} &= \text{Toeplitz}([1, r, \dots, r^{d-1}]) \\ &= \begin{bmatrix} 1 & r & r^2 & \dots & r^{d-1} \\ r & 1 & r & \dots & r^{d-2} \\ \vdots & \vdots & \ddots & & \vdots \\ r^{d-1} & r^{d-2} & \dots & & 1 \end{bmatrix} \end{aligned} \quad (10)$$

Here  $r \triangleq \text{sign}(\frac{m_1}{m_0}) \min\{|\frac{m_1}{m_0}|, 0.99\}$ , where  $m_0$  is the average of the elements along the main diagonal and  $m_1$  the average of the elements along the main sub-diagonal of the matrix  $\mathbf{B}$  in (9). 0.99 is a bound such that  $r$  has a reasonable value. This correlation matrix corresponds to modeling the block elements by a first order Auto-Regressive (AR) process. When blocks have different sizes, the above idea can still be used. First, using the EM method we can derive the rule for each  $\mathbf{B}_i$ :

$$\mathbf{B}_i \leftarrow \frac{1}{\gamma_i} [\Sigma_x^i + \mu_x^i (\mu_x^i)^T].$$

Then, for each  $\mathbf{B}_i$  we calculate the means of the elements along the main diagonal and the main sub-diagonal, i.e.  $m_0^i$  and  $m_1^i$ , respectively. Next, evaluate the averaged values:  $\bar{m}_0 \triangleq \sum_{i=1}^g m_0^i$  and  $\bar{m}_1 \triangleq \sum_{i=1}^g m_1^i$ . Finally, we have  $\bar{r} \triangleq \text{sign}(\frac{\bar{m}_1}{\bar{m}_0}) \min\{|\frac{\bar{m}_1}{\bar{m}_0}|, 0.99\}$ , from which we construct  $\hat{\mathbf{B}}_i$  for the  $i$ -th block with the similar form in (10), i.e.

$$\hat{\mathbf{B}}_i = \text{Toeplitz}([1, \bar{r}, \dots, \bar{r}^{d_i-1}]). \quad (11)$$

We denote the above algorithm by **BSBL-EM**.

### B. BSBL-BO: the Bound-Optimization Method

The derived BSBL-EM has good recovery performance but has slow speed. Now we derive another algorithm, which not only has satisfying recovery performance but has faster speed as well. The algorithm is based on the bound-optimization method (also known as Majorization-Minimization (MM) method) [15]–[17].

Note that the original cost function (5) consists of two terms. The first term  $\log |\lambda \mathbf{I} + \Phi \Sigma_0 \Phi^T|$  is concave with respect to  $\gamma \succeq \mathbf{0}$ , where we denote  $\gamma \triangleq [\gamma_1, \dots, \gamma_g]^T$ . The second term  $\mathbf{y}^T (\lambda \mathbf{I} + \Phi \Sigma_0 \Phi^T)^{-1} \mathbf{y}$  is convex with respect to  $\gamma \succeq \mathbf{0}$ . Since our goal is to minimize the cost function, we choose to find an upper-bound for the first item and then minimize the upper-bound. We use the supporting hyperplane of the first term as its upper-bound. Let  $\gamma^*$  be a given point in the  $\gamma$ -space. We have

$$\begin{aligned} \log |\lambda \mathbf{I} + \Phi \Sigma_0 \Phi^T| &\leq \log |\lambda \mathbf{I} + \Phi \Sigma_0^* \Phi^T| \\ &\quad + \sum_{i=1}^g \text{Tr}((\Sigma_y^*)^{-1} \Phi^i \mathbf{B}_i (\Phi^i)^T) (\gamma_i - \gamma_i^*) \\ &= \sum_{i=1}^g \text{Tr}((\Sigma_y^*)^{-1} \Phi^i \mathbf{B}_i (\Phi^i)^T) \gamma_i + \log |\Sigma_y^*| \\ &\quad - \sum_{i=1}^g \text{Tr}((\Sigma_y^*)^{-1} \Phi^i \mathbf{B}_i (\Phi^i)^T) \gamma_i^* \end{aligned} \quad (12)$$

where  $\Sigma_y^* = \lambda \mathbf{I} + \Phi \Sigma_0^* \Phi^T$  and  $\Sigma_0^* = \Sigma_0|_{\gamma=\gamma^*}$ . Substituting (12) into the cost function (5) we have

$$\begin{aligned} \mathcal{L}(\gamma) &\leq \sum_{i=1}^g \text{Tr}((\Sigma_y^*)^{-1} \Phi^i \mathbf{B}_i (\Phi^i)^T) \gamma_i \\ &\quad + \mathbf{y}^T (\lambda \mathbf{I} + \Phi \Sigma_0 \Phi^T)^{-1} \mathbf{y} + \log |\Sigma_y^*| \\ &\quad - \sum_{i=1}^g \text{Tr}((\Sigma_y^*)^{-1} \Phi^i \mathbf{B}_i (\Phi^i)^T) \gamma_i^* \\ &\triangleq \tilde{\mathcal{L}}(\gamma) \end{aligned} \quad (13)$$

The function  $\tilde{\mathcal{L}}(\gamma)$  is convex over  $\gamma$  and when  $\gamma = \gamma^*$ , we have  $\mathcal{L}(\gamma^*) = \tilde{\mathcal{L}}(\gamma^*)$ . Further, for any  $\gamma_{\min}$  which is the minimum point of  $\tilde{\mathcal{L}}(\gamma)$ , we have the following relationship

$$\mathcal{L}(\gamma_{\min}) \leq \tilde{\mathcal{L}}(\gamma_{\min}) \leq \tilde{\mathcal{L}}(\gamma^*) = \mathcal{L}(\gamma^*).$$

This relationship indicates that when we minimize the surrogate function  $\tilde{\mathcal{L}}(\gamma)$  over  $\gamma$ , the resulting minimum point effectively decreases the original cost function  $\mathcal{L}(\gamma)$ . We can use any convex optimization software to optimize the function (13). However, this takes more time than BSBL-EM and experiments

have shown that also leads to poorer recovery performance. Therefore, we consider other surrogate functions. Using the identity:

$$\mathbf{y}^T(\lambda\mathbf{I} + \Phi\Sigma_0\Phi^T)^{-1}\mathbf{y} \equiv \min_{\mathbf{x}} \left[ \frac{1}{\lambda} \|\mathbf{y} - \Phi\mathbf{x}\|_2^2 + \mathbf{x}^T \Sigma_0^{-1} \mathbf{x} \right] \quad (14)$$

we have

$$\begin{aligned} \tilde{\mathcal{L}}(\gamma) &= \min_{\mathbf{x}} \frac{1}{\lambda} \|\mathbf{y} - \Phi\mathbf{x}\|_2^2 + \mathbf{x}^T \Sigma_0^{-1} \mathbf{x} \\ &\quad + \sum_{i=1}^g \text{Tr}((\Sigma_y^*)^{-1} \Phi^i \mathbf{B}_i (\Phi^i)^T) \gamma_i + \log |\Sigma_y^*| \\ &\quad - \sum_{i=1}^g \text{Tr}((\Sigma_y^*)^{-1} \Phi^i \mathbf{B}_i (\Phi^i)^T) \gamma_i^*. \end{aligned}$$

Then, a new function

$$\begin{aligned} \mathcal{G}(\gamma, \mathbf{x}) &\triangleq \frac{1}{\lambda} \|\mathbf{y} - \Phi\mathbf{x}\|_2^2 + \mathbf{x}^T \Sigma_0^{-1} \mathbf{x} \\ &\quad + \sum_{i=1}^g \text{Tr}((\Sigma_y^*)^{-1} \Phi^i \mathbf{B}_i (\Phi^i)^T) \gamma_i \\ &\quad + \log |\Sigma_y^*| - \sum_{i=1}^g \text{Tr}((\Sigma_y^*)^{-1} \Phi^i \mathbf{B}_i (\Phi^i)^T) \gamma_i^* \end{aligned}$$

is defined, which is the upper-bound of  $\tilde{\mathcal{L}}(\gamma)$ . Note that  $\mathcal{G}(\gamma, \mathbf{x})$  is convex in both  $\gamma$  and  $\mathbf{x}$ . It can be easily shown that the solution  $(\gamma^\diamond)$  of  $\tilde{\mathcal{L}}(\gamma)$  is the solution  $(\gamma^\diamond, \mathbf{x}^\diamond)$  of  $\mathcal{G}(\gamma, \mathbf{x})$ . Thus,  $\mathcal{G}(\gamma, \mathbf{x})$  is our final surrogate cost function.

Taking the derivative of  $\mathcal{G}$  with respect to  $\gamma_i$  and  $\mathbf{x}$ , respectively, we can obtain

$$\gamma_i \leftarrow \sqrt{\frac{\mathbf{x}_i^T \mathbf{B}_i^{-1} \mathbf{x}_i}{\text{Tr}((\Phi^i)^T (\Sigma_y^*)^{-1} \Phi^i \mathbf{B}_i)}} \quad (15)$$

$$\mathbf{x} \leftarrow \Sigma_0 \Phi^T (\lambda \mathbf{I} + \Phi \Sigma_0 \Phi^T)^{-1} \mathbf{y}. \quad (16)$$

Note (16) is the same as (3). The learning rules for  $\lambda$  can be directly derived from (5) using the gradient method, which is the same as (7). Similarly, in low SNR cases, we choose the robust rule (8). The learning rule for  $\mathbf{B}_i$  can be derived in the same manner as the BSBL-EM. Using the same constraint as in BSBL-EM to overcome the overfitting, we have the same learning rule (10) if blocks have the same size, or the one in (11) if blocks have different sizes

We call this algorithm **BSBL-BO**. Compared to BSBL-EM, this algorithm is much faster while its performance is close to BSBL-EM.



### C. BSBL- $\ell_1$ : Hybrid of BSBL and Group-Lasso Type Algorithms

Since the cost function of BSBL-EM and BSBL-BO is a function of  $\gamma$ , they essentially operate in the  $\gamma$ -space. In contrast, most existing algorithms for the model (1)-(2) directly operate in the  $\mathbf{x}$ -space, minimizing a data fit term and a penalty that are both functions of  $\mathbf{x}$ . It is interesting to see the relation between our bSBL algorithms and those existing algorithms. Such connection can not only provide insights into how to modify existing algorithms to exploit intra-block correlation for better performance, but also lead to bSBL algorithm variants that have faster convergence.

Using the idea we presented in [18], an extension of the duality space analysis of the basic SBL framework [19], we can transform the bSBL cost function (5) from the  $\gamma$ -space to the  $\mathbf{x}$ -space. Since the transformation is obtained by closely following the method in [18], [19], here we only present the key steps to enhance readability and context.

First, using the identity (14) we can upper-bound the bSBL cost function as follows

$$\mathcal{L}(\mathbf{x}, \gamma) = \log |\lambda \mathbf{I} + \Phi \Sigma_0 \Phi^T| + \frac{1}{\lambda} \|\mathbf{y} - \Phi \mathbf{x}\|_2^2 + \mathbf{x}^T \Sigma_0^{-1} \mathbf{x}.$$

By first minimizing over  $\gamma$  and then minimizing over  $\mathbf{x}$ , we have:

$$\mathbf{x} = \arg \min_{\mathbf{x}} \left\{ \|\mathbf{y} - \Phi \mathbf{x}\|_2^2 + \lambda g_c(\mathbf{x}) \right\}, \quad (17)$$

where  $g_c(\mathbf{x}) \triangleq \min_{\gamma \succeq \mathbf{0}} \left\{ \mathbf{x}^T \Sigma_0^{-1} \mathbf{x} + \log |\lambda \mathbf{I} + \Phi \Sigma_0 \Phi^T| \right\}$ . Using the fact that  $h(\gamma) \triangleq \log |\lambda \mathbf{I} + \Phi \Sigma_0 \Phi^T|$  is concave and non-decreasing w.r.t.  $\gamma \succeq \mathbf{0}$ , the penalty  $g_c(\mathbf{x})$  can be transformed to

$$g_c(\mathbf{x}) = \min_{\mathbf{z} \succeq \mathbf{0}} \sum_i \left( 2z_i^{\frac{1}{2}} \sqrt{\mathbf{x}_i^T \mathbf{B}_i^{-1} \mathbf{x}_i} \right) - h^*(\mathbf{z}), \quad (18)$$

where  $\mathbf{z} = [z_1, \dots, z_g]^T$ ,  $h^*(\mathbf{z})$  is the concave conjugate of  $h(\gamma)$  and can be expressed as  $h^*(\mathbf{z}) = \min_{\gamma \succeq \mathbf{0}} \mathbf{z}^T \gamma - \log |\lambda \mathbf{I} + \Phi \Sigma_0 \Phi^T|$ .

Now consider the problem (17) with the regularization term (18). Using the duality relation between  $\mathbf{z}$  and  $\gamma$ , we can calculate the optimal value for  $\mathbf{z}$ . This leads to the iterative reweighted algorithm

$$\mathbf{x}^{(k+1)} = \arg \min_{\mathbf{x}} \|\mathbf{y} - \Phi \mathbf{x}\|_2^2 + \lambda \sum_i w_i^{(k)} \sqrt{\mathbf{x}_i^T \mathbf{B}_i^{-1} \mathbf{x}_i} \quad (19)$$

$$w_i^{(k)} = \left( \text{Tr} [\mathbf{B}_i \Phi_i^T (\lambda \mathbf{I} + \Phi \Sigma_0^{(k)} \Phi^T)^{-1} \Phi_i] \right)^{\frac{1}{2}}$$

$$\Sigma_0^{(k)} = \text{diag} \{ \gamma_1^{(k)} \mathbf{B}_1, \dots, \gamma_g^{(k)} \mathbf{B}_g \}$$

$$\gamma_i^{(k)} = 2 \sqrt{(\mathbf{x}_i^{(k)})^T \mathbf{B}_i^{-1} (\mathbf{x}_i^{(k)})} / w_i^{(k-1)}$$

The solution to (19) can be calculated using any group-Lasso type algorithms. To see this, letting  $\mathbf{u}_i \triangleq (w_i^{(k)})^2 \mathbf{B}_i^{-1/2} \mathbf{x}_i$  and  $\mathbf{H} \triangleq \Phi \cdot \text{diag}\{\mathbf{B}_1^{1/2}/(w_1^{(k)})^2, \dots, \mathbf{B}_g^{1/2}/(w_g^{(k)})^2\}$ , the problem (19) can be transformed to the following one

$$\mathbf{u}^{(k+1)} = \arg \min_{\mathbf{u}} \|\mathbf{y} - \mathbf{H}\mathbf{u}\|_2^2 + \lambda \sum_i \|\mathbf{u}_i\|_2,$$

where  $\mathbf{u} = [\mathbf{u}_1^T, \dots, \mathbf{u}_g^T]^T$ . Each iteration is a standard group-Lasso type problem, with each iteration providing a block sparse solution, while the whole algorithm is an iterative reweighted algorithm. In the above development, we did not consider the learning rules for the regularizer  $\lambda$  and  $\mathbf{B}_i$ . In fact, their computation greatly benefits from this iterative reweighted form. Since each iteration is a group-Lasso type problem, the optimal value of  $\lambda$  can be automatically selected in the group Lasso framework [20]. Also, since each iteration provides a block-sparse solution, which is close to the true solution, we can directly calculate  $\mathbf{B}_i$  from the solution of the previous iteration with the strategy to overcome overfitting as before. For example, in each iteration we can model elements of every block as a first-order AR process with a common coefficient, and then calculate the coefficient and finally construct each  $\mathbf{B}_i$ . We call this algorithm **BSBL- $\ell_1$** .

Now we discuss the connection of BSBL- $\ell_1$  to existing algorithms. When we do not consider the intra-block correlation (i.e. setting  $\mathbf{B}_i = \mathbf{I}$ ) and also do not iterate the algorithm, BSBL- $\ell_1$  reduces to the canonical group Lasso algorithm [1]. When we iterate the algorithm but ignore the intra-block correlation, the algorithm reduces to the block version of the iterative reweighted  $\ell_1$  algorithm [16]. The algorithm can also be viewed as one employing kernel regularization and  $\mathbf{B}_i$  is a *data-adaptive* kernel, which is advantageous to those using user-defined kernels such as Radius Basis kernels [21].

BSBL- $\ell_1$  can be seen as a hybrid of bSBL algorithms and group-Lasso type algorithms. From one side, it has the ability to adaptively learn and exploit the intra-block correlation for better performance, as BSBL-EM and BSBL-BO. From the other side, since it only takes few iterations<sup>2</sup> and each iteration can be implemented by efficient group-Lasso type algorithms, it is much faster and is especially suitable for large-scale data sets, compared to BSBL-EM and BSBL-BO. The algorithm also provides insights if we want to equip group-Lasso type algorithms with the ability to exploit intra-block correlation for better recovery performance. We can consider the iterative reweighted method and change the  $\ell_2$  norm,  $\|\mathbf{x}_i\|_2$ , to the Mahalanobis-distance type measure,  $\sqrt{\mathbf{x}_i^T \mathbf{B}_i^{-1} \mathbf{x}_i}$ .

<sup>2</sup>In our experiments it only took about two iterations in noisy cases.

#### IV. ALGORITHMS FOR UNKNOWN BLOCK PARTITION

Now we extend the algorithmic framework to derive algorithms when the block partition is unknown. We start with our model motivated by the physics of certain applications and show that with proper interpretation it has considerable flexibility and generality. This model is consistent with communication channel modeling where an ideal sparse channel consisting of a few specular multi-path components has a discrete-time, bandlimited, baseband representation, which exhibits a block sparse structure with the block centers determined by the arbitrary arrival times of the multi-path components. Since the blocks are arbitrarily located they can overlap giving rise to larger unequal blocks. For the algorithm development, *we assume that all the blocks are of equal size  $h$  and that the non-zeros blocks are arbitrarily located.* Later we will see that the approximation of equal block-size is not limiting. Note that though the resulting algorithm is not very sensitive to the choice of  $h$ , algorithmic performance can be further improved if a suitable value of  $h$  is selected. We will comment more on  $h$  later.

##### A. Model Description and Algorithms

Given the identical block size  $h$ , there are  $p \triangleq N - h + 1$  possible blocks in  $\mathbf{x}$ , which overlap each other. The  $i$ -th block starts at the  $i$ -th element of  $\mathbf{x}$  and ends at the  $(i + h - 1)$ -th element. All the nonzero elements of  $\mathbf{x}$  lie in some of these blocks. Similar to Section III, for the  $i$ -th block, we assume it satisfies a multivariate Gaussian distribution with the mean given by  $\mathbf{0}$  and the covariance matrix given by  $\gamma_i \mathbf{B}_i$ , where  $\mathbf{B}_i \in \mathbb{R}^{h \times h}$ . So we have the prior of  $\mathbf{x}$  as the form:  $p(\mathbf{x}) \sim \mathcal{N}_x(\mathbf{0}, \Sigma_0)$ . Note that due to the overlapping of these blocks, here  $\Sigma_0$  is no longer a block diagonal matrix. It has the structure that each  $\gamma_i \mathbf{B}_i$  lies along the principal diagonal of  $\Sigma_0$  and overlaps other  $\gamma_j \mathbf{B}_j$  in neighbor (see the left picture in Fig.1). Starting with this model we can develop algorithms for estimating the hyper-parameters  $\lambda, \{\gamma_i, \mathbf{B}_i\}_{i=1}^p$ . However, because the covariance matrix  $\Sigma_0$  is no longer a block diagonal matrix we cannot directly use the bSBL framework and need to make some modifications.

To facilitate the use of the bSBL framework, we expand the covariance matrix  $\Sigma_0$  as follows:

$$\tilde{\Sigma}_0 = \text{diag}\{\gamma_1 \mathbf{B}_1, \dots, \gamma_p \mathbf{B}_p\} \in \mathbb{R}^{ph \times ph} \quad (20)$$

Note that now  $\gamma_i \mathbf{B}_i$  does not overlap other  $\gamma_j \mathbf{B}_j (i \neq j)$  (see the right picture in Fig.1). The expanded covariance matrix  $\tilde{\Sigma}_0$  implies the decomposition of  $\mathbf{x}$ :

$$\mathbf{x} = \sum_{i=1}^p \mathbf{E}_i \mathbf{z}_i, \quad (21)$$

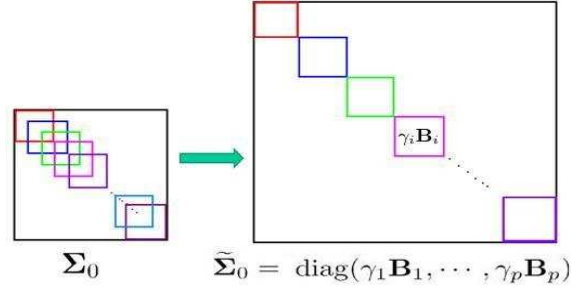


Fig. 1. Structures of the original  $\Sigma_0$  and the expanded  $\tilde{\Sigma}_0$ . Each color block corresponds to a possible nonzero block in  $\mathbf{x}$ .

where  $E\{\mathbf{z}_i\} = \mathbf{0}$ ,  $E\{\mathbf{z}_i \mathbf{z}_j^T\} = \delta_{i,j} \gamma_i \mathbf{B}_i$  ( $\delta_{i,j} = 1$  if  $i = j$ ; otherwise,  $\delta_{i,j} = 0$ ), and  $\mathbf{z} \triangleq [\mathbf{z}_1^T, \dots, \mathbf{z}_p^T]^T \sim \mathcal{N}_{\mathbf{z}}(\mathbf{0}, \tilde{\Sigma}_0)$ .  $\mathbf{E}_i \in \mathbb{R}^{M \times h}$  is a zero matrix except that the part from its  $i$ -th row to  $(i + h - 1)$ -th row is replaced by the identity matrix  $\mathbf{I}$ . Then the original model (1) can be expressed as:

$$\mathbf{y} = \sum_{i=1}^p \Phi \mathbf{E}_i \mathbf{z}_i + \mathbf{v} \triangleq \mathbf{A} \mathbf{z} + \mathbf{v}, \quad (22)$$

where  $\mathbf{A} \triangleq [\mathbf{A}_1, \dots, \mathbf{A}_p]$  with  $\mathbf{A}_i \triangleq \Phi \mathbf{E}_i$ . Now we see the new model (22) is exactly a bSBL model.

Therefore, straightforwardly following the development of BSBL-EM, BSBL-BO, and BSBL- $\ell_1$ , we can derive algorithms for this expanded model, which are called **EBSBL-EM**, **EBSBL-BO**, and **EBSBL- $\ell_1$** , respectively.

### B. Flexibility of the Expanded Model

In the above development, we assumed that all the blocks have the same size  $h$ , which is known. However, this assumption is not crucial for practical use. When the size of a nonzero block of  $\mathbf{x}$ , say  $\mathbf{x}_j$ , is larger or equal to  $h$ , it can be recovered by a set of (overlapped)  $\mathbf{z}_i$  ( $i \in \mathcal{S}$ ,  $\mathcal{S}$  is a non-empty set). When the size of  $\mathbf{x}_j$  is smaller than  $h$ , it can also be recovered by a  $\mathbf{z}_i$  for some  $i$ . In this case, since  $\mathbf{z}_i$  is larger, the elements of  $\mathbf{z}_i$  with global locations (i.e. the indexes in  $\mathbf{x}$ ) different to those of elements of  $\mathbf{x}_j$  are very close to zero. In Section V-C, we will see different values of  $h$  lead to similar performance. In fact, the parameter  $h$  can be better viewed as a regularizer, balancing recovery quality and computational load (larger  $h$  increases computational load).

The above insight implies that we can also use the BSBL-EM, BSBL-BO or BSBL- $\ell_1$  in this situation. We can partition a signal into blocks of equal (or almost equal) size  $h$ . And  $h$  serves as a regularizer again. In Section V-C we will empirically verify this idea.

Note that our approach using the expanded model in the situation when block partition is unknown is quite different to existing approaches [6], [7]. An obvious advantage of our approach is that it simplifies algorithms, which, in turn, increases their robustness in noisy environments, as shown in Section V-C. Another benefit of this approach is that it facilitates the exploitation of intra-block correlation. As we will see, exploiting intra-block correlation can significantly improve algorithms' performance. Since in practice such intra-block correlation widely exists, our approach is more competitive than existing approaches.

## V. EXPERIMENTS

Due to space limit, we show only some representative experiment results. We compare our proposed algorithms to Group Lasso [1], Mixed  $\ell_2/\ell_1$  Program [5], Group Basis Pursuit [4], Block-OMP [3], Block-CoSaMp [2], StructOMP [6], CluSS-MCMC [7], and BM-MAP-OMP [8], most of which show top performance in published algorithm comparisons. And we use the T-MSBL algorithm [9] as a benchmark in the experiment when any a priori knowledge on the blocks is unavailable. Note that when T-MSBL, initially proposed for the MMV model, is used in the block sparse model (1)-(2), it can be viewed as a special case of BSBL-EM with each block size being 1. We also calculate the 'oracle' result, which is the least-square estimate of  $\mathbf{x}$  given its true support. As for our BSBL- $\ell_1$ , we use the SGPL1 software [4] (in noisy cases) or the Mixed  $\ell_2/\ell_1$  Program (in noiseless cases) to implement each iteration. For every set of experiment settings, our experiment consists of 500 trials. The matrix  $\Phi$  in all the experiments are generated as zero mean random Gaussian matrices with columns normalized to unit  $\ell_2$  norm. In noisy experiments we use the normalized mean square error (NMSE) as a performance index, defined by  $\|\hat{\mathbf{x}} - \mathbf{x}\|_2^2 / \|\mathbf{x}\|_2^2$ , where  $\hat{\mathbf{x}}$  is the estimate of the true signal  $\mathbf{x}$ . In noiseless experiments we choose the Success Rate as a performance index, defined as the percentage of successful trials in the 500 trials. A successful trial is defined as the one when the NMSE is less than  $10^{-6}$ .

### A. Experiments: When Block Partition is Known

We compare our algorithms to Block-OMP, Block-CoSaMP (given the number of nonzero blocks), Mixed  $\ell_2/\ell_1$  Programm, Group Lasso (using the continuation method <sup>3</sup>), and Group Basis Pursuit when a priori knowledge on block partition is available. We first consider noiseless cases. In each trial we generated a block-sparse signal of length 512. It was partitioned into blocks with identical size 8. Ten

<sup>3</sup>Namely, it iterates many times. In each iteration, starting from the solution of the previous iteration, it searches a new solution and chooses a slightly smaller value for  $\lambda$ .

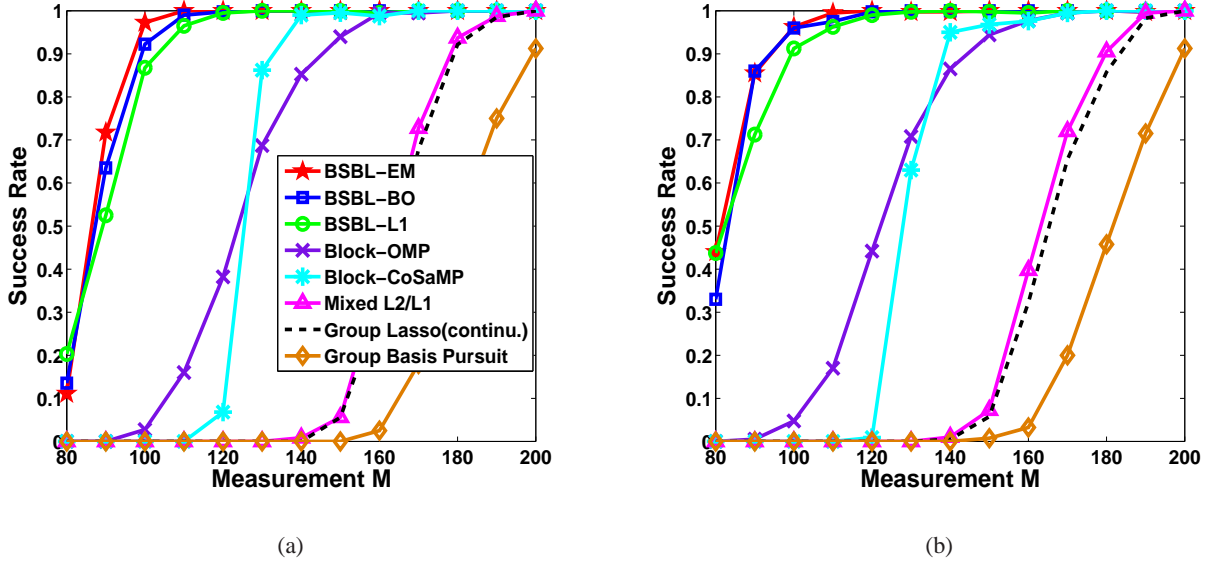


Fig. 2. Algorithm comparison in noiseless cases when correlation in each block was (a) zero or (b) uniformly chosen from 0.9 to 1.

blocks were nonzero (randomly chosen). The matrix  $\Phi$  was of the size  $M \times 512$ , where  $M$  varied from 80 to 200. We consider two situations. One is that the correlation in each block was zero; the other situation is the correlation in each block was uniformly chosen from 0.9 to 1. The corresponding results are shown in Fig.2 (a) and (b). We can see our proposed BSBL-EM, BSBL-BO, and BSBL- $\ell_1$  had much better performance in both situations. Note that when the intra-block correlation changed from low value to high value, our proposed algorithms had significantly improved performance, while other algorithms' performance was almost unchanged or slightly worse. In Experiment 3 we will more clearly see this phenomenon.

Next, we study these algorithms' performance at different noise levels. The matrix  $\Phi$  was of the size  $128 \times 512$ . The block size and the block partition were the same as before. Seven blocks were nonzero with intra-block correlation uniformly chosen from 0.8 to 1. Gaussian white noise was added such that the SNR, defined by  $\text{SNR}(\text{dB}) \triangleq 20 \log_{10}(\|\Phi \mathbf{x}_{\text{gen}}\|_2 / \|\mathbf{v}\|_2)$ , varied from 5 dB to 25 dB. Since Block-CoSaMP and Block-OMP are only suitable for noiseless cases, we didn't compare them. The results are shown in Fig.3 (a). Again, we see our algorithms had much better performance than the compared ones, especially the performance curves of BSBL-EM and BSBL-BO almost overlapped the 'Oracle' performance curve. Note that the slightly worse performance of BSBL- $\ell_1$  at 5dB and 25dB is due to some pre-defined parameters in the used SGLP1 software. When we changed other software we could

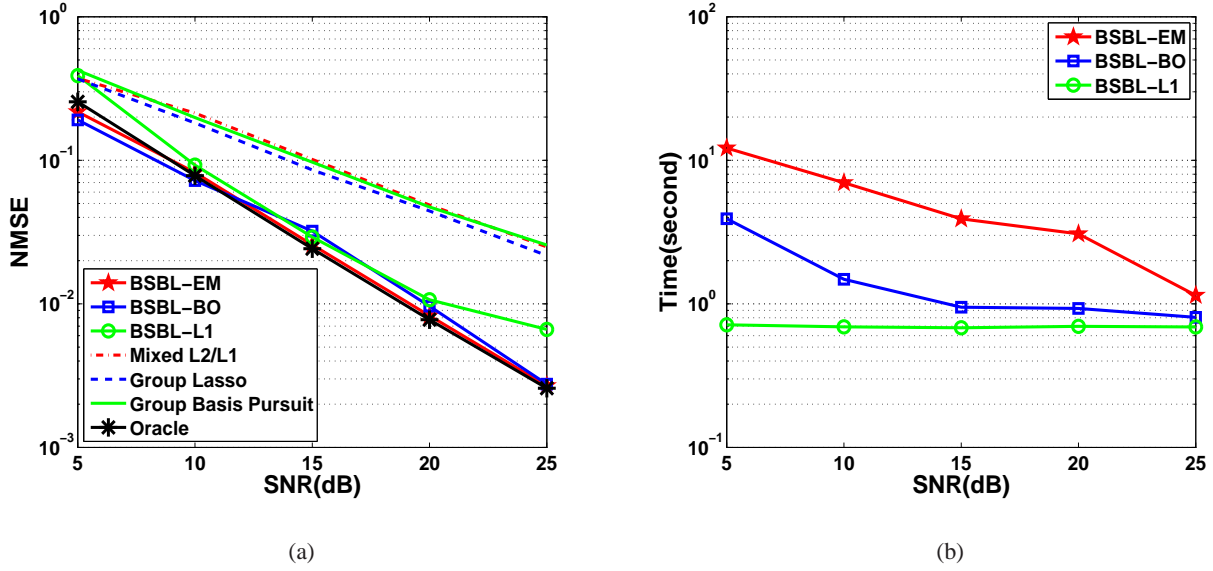


Fig. 3. (a) Performance comparison in noisy cases when correlation in each block was uniformly chosen from 0.8 to 1. (b) Speed comparison of the three proposed algorithms in the experiment in (a).

get better performance at these two noise levels. Figure 3 (b) gives the speed comparison of the three algorithms. Clearly, BSBL- $\ell_1$  was the fastest.

### B. Experiments: Effects of Intra-Block Correlation

We now study the effects of intra-block correlation. To highlight the role of correlation, we carry out experiments with no noise. The matrix  $\Phi$  was of the size  $100 \times 300$ . The sparse signal consisted of 75 blocks with identical size. Only 20 of the blocks were nonzero. All the nonzero blocks were generated from the same multivariate Gaussian distribution:  $\mathcal{N}(\mathbf{0}, \Sigma)$ , where  $\Sigma$  was generated using the Matlab command: `Toeplitz([1,  $\beta$ ,  $\dots$ ,  $\beta^3$ ])`.  $\beta$  assumed values from -0.99 to 0.99. Note that  $\beta$  is the parameter measuring the intra-block correlation. BSBL-EM was performed in three ways. First, it adaptively learned and exploited the intra-block correlation. In the second case, it was given the true intra-block correlation (i.e. set  $\mathbf{B} = \Sigma$ ). In the third case, it ignored the correlation (i.e. set  $\mathbf{B} = \mathbf{I}$ ).

The results are shown in Fig.4 (a), from which we have two observations. First, we can see that **exploiting the intra-block correlation greatly improved the performance of BSBL-EM**. BSBL-BO and BSBL- $\ell_1$  have similar performance, as shown in the figure. Second, **when not exploiting the intra-block correlation, the performance of the three algorithms was almost not affected by the correlation values** (for clear display, we only show the performance of BSBL-EM). Note that the second

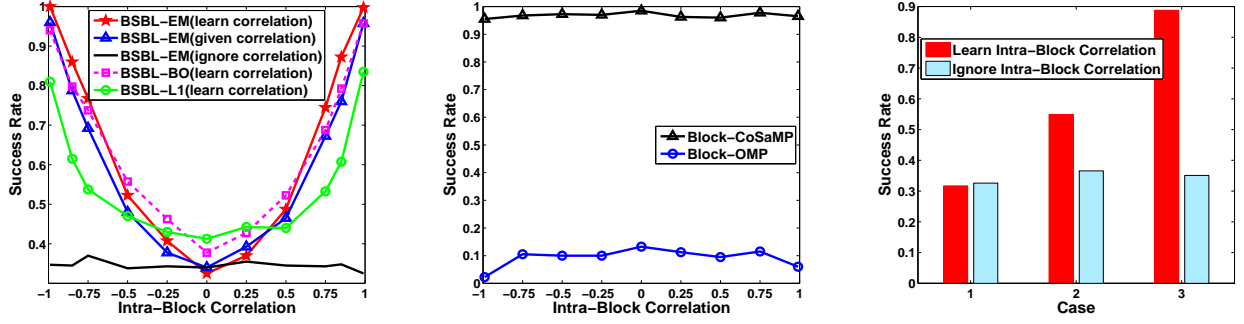


Fig. 4. The effect of intra-block correlation on the recovery performance of the proposed algorithms (left figure) and of Block-OMP and Block-CoSaMP (middle figure). Experiment settings in the two figures were different. The right figure shows the performance of BSBL-EM in three correlation cases.

observation is different from the observation on *temporal* correlation in the MMV model, where we found that if temporal correlation is not exploited, algorithms have poorer performance with increasing temporal correlation values [9]. The second observation can also be seen from existing algorithms. In Fig.4 (b) we plot the performance of Block-OMP and Block-CoSaMP as two examples (With the above experiment settings the two algorithms had zero success rate. So we reduced the number of nonzero blocks to 15, making the inverse problem much easier.). We can see the intra-block correlation had little effects on their performance.

In the above experiment all the nonzero blocks had almost the same intra-block correlation. A nature question is when different nonzero blocks have largely different intra-block correlation values, can our proposed algorithms still exploit the correlation to improve performance? To answer it, we consider three correlation cases. In the first case the intra-block correlation of each nonzero block was uniformly chosen from -1 to 1; in the second case, uniformly chosen from 0 to 1; and in the third case, uniformly chosen from 0.7 to 1. BSBL-EM was performed in two ways, i.e. exploiting correlation and ignoring correlation. The averaged results corresponding to the three cases are shown in Fig.4 (c), indicated by ‘Case 1’, ‘Case 2’, and ‘Case 3’, respectively. We can see in Case 3 the benefit from exploiting the correlation was significant, while in Case 1 the benefit disappeared (but exploiting correlation was not harmful). However, note that the Case 1 rarely happens in practice. In fact, in many practical problems the intra-block correlation of all nonzero blocks tends to be positive (if elements in a block are modeled as an AR(1) process) and high, which corresponds to Case 2 and Case 3.



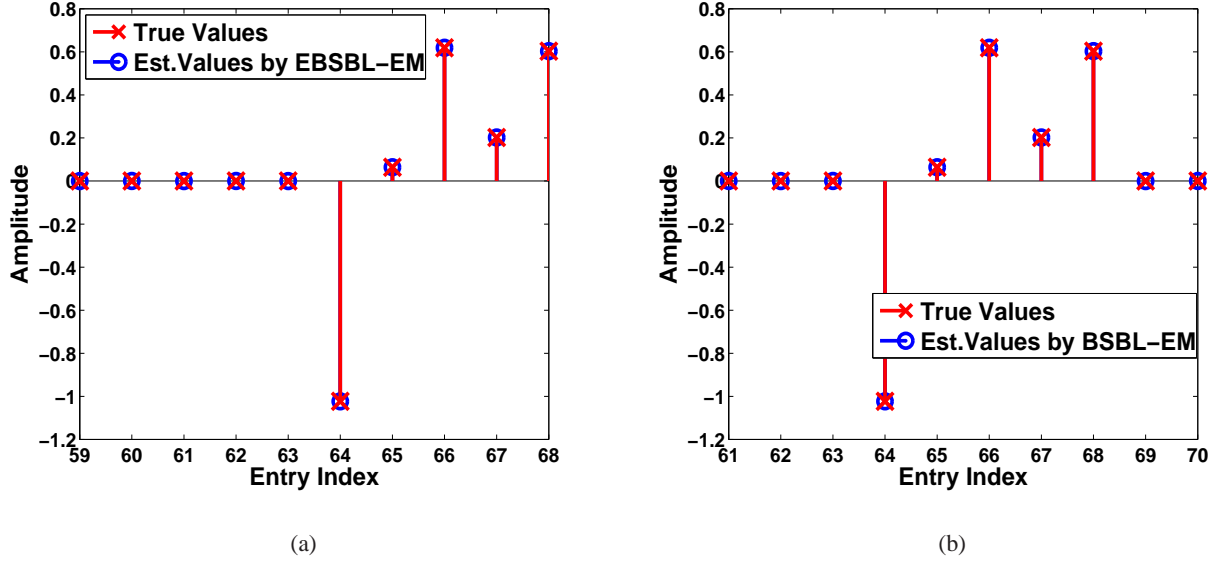


Fig. 5. (a) A nonzero block in  $\mathbf{x}$  consisting of 5 elements was reconstructed by EBSBL-EM with  $h = 10$ . (b) The same block was reconstructed by BSBL-EM.

### C. Experiments: When Block Partition is Unknown

In Section IV-B we stated that the assumption of identical block size is not crucial. Here we give experiments to support our claim. We first consider a noiseless experiment. The matrix  $\Phi$  was of the size  $192 \times 512$ . The signal  $\mathbf{x}$  had  $g$  nonzero blocks with random size and random locations (not overlapping).  $g$  was varied from 2 to 10. The total number of nonzero elements in  $\mathbf{x}$  was fixed to 48.

We randomly pick a trial for illustration. In this trial,  $\mathbf{x}$  was recovered by EBSBL-EM with  $h = 10$ . We take a nonzero block of  $\mathbf{x}$  with indexes from 64 to 68 for example (see Fig.5(a)). These indexes are denoted by  $\mathcal{I}_{\text{true}}$ . Corresponding to this block in the recovered signal is a segment with indexes from 59 to 68 (since  $h = 10$ ), which comes from an estimated  $\mathbf{z}_i$  with some  $i$ . Denote the indexes of the segment by  $\mathcal{I}_{\text{est}}$ , where  $\mathcal{I}_{\text{est}} = \{59, 60, \dots, 68\}$ . Figure 5(a) shows elements in this segment with indexes  $\mathcal{I}_{\text{true}}$  were almost the same as elements in the true block, while elements in this segment with indexes not in  $\mathcal{I}_{\text{true}}$  were almost zero. Denote by  $\hat{\mathbf{s}}$  the segment in the recovered signal with indexes  $\mathcal{I}_{\text{est}}$ , and by  $\mathbf{s}$  the segment in the true signal with the same indexes  $\mathcal{I}_{\text{est}}$ . The Euclidean distance between  $\hat{\mathbf{s}}$  and  $\mathbf{s}$  is calculated as  $\|\hat{\mathbf{s}} - \mathbf{s}\|_2^2 = 3.8982 \times 10^{-14}$ , indicating ‘no difference’ between  $\hat{\mathbf{s}}$  and  $\mathbf{s}$ .

In Section IV-B we also pointed out that we can use the BSBL-EM, BSBL-BO or BSBL- $\ell_1$  here. We use BSBL-EM as an illustration. We defined a partition of  $\mathbf{x}$  for BSBL-EM. The blocks were almost

evenly partitioned such that each block's first element located at  $\{1, 11, 21, \dots, 501, 511\}$ . Figure 5(b) shows the same nonzero block in the above experiment recovered by BSBL-EM. Due to the defined partition, corresponding to the nonzero block is a segment in the recovered signal with indexes from 61 to 70. Again, we observe the nonzero block was perfectly recovered. Denote by  $\tilde{\mathbf{t}}$  the segment in the recovered signal, and by  $\mathbf{t}$  the corresponding segment in the original signal  $\mathbf{x}$ . Their Euclidean distance is calculated as  $\|\tilde{\mathbf{t}} - \mathbf{t}\|_2^2 = 5.5388 \times 10^{-27}$ , indicating no difference between them.

Next, we set up a noisy experiment when block partition is unknown and compare our algorithms with three recently proposed algorithms; StructOMP (given the number of nonzero elements), BM-MAP-OMP (given the true noise variance), and CluSS-MCMC. As we stated in Section IV-B,  $h$  is not crucial for practical use. To see this, we set  $h = 4$  and  $h = 8$  for our algorithms. But to prevent from being overcrowded when plotting performance curves, we only display BSBL-EM and EBSBL-BO with  $h = 4$  and  $h = 8$ . We also perform T-MSBL here. As stated before, T-MSBL serves as a benchmark, by which we can see what result we can get if we do not consider exploring and exploiting block partition information. If an algorithm, designed to explore and exploit block partition information, has poorer performance than T-MSBL, we may consider to use T-MSBL instead of it.

The experiment settings were the same as above, except that SNR was 15 dB. The results are shown in Fig.6. We can see our algorithms outperformed StructOMP, CluSS-MCMC, and BM-MAP-OMP. We also observe that for either BSBL-EM or EBSBL-BO, setting  $h = 4$  or  $h = 8$  led to similar performance. But note that if one can roughly know the nonzero block sizes, better performance can be reached by choosing a suitable value for  $h$ . For example, in this experiment when the group number is small (i.e. each nonzero block size is large in average), one can choose larger value for  $h$  for better performance. Besides, we see even T-MSBL outperformed StructOMP, CluSS-MCMC, and BM-MAP-OMP when the group number became larger.

## VI. CONCLUSION

Based on the block sparse Bayesian learning framework and its extension, we proposed a number of algorithms for the block sparse model in the cases when block partition is known, when block partition is unknown but nonzero block sizes are known, and when any a priori knowledge is unavailable. These algorithms are shown to have superior performance compared to existing algorithms. Although not shown, our algorithms also have superior performance for the case when blocks overlap. Since the multiple measurement vector model [9] can be seen as a special model of the block sparse model, our proposed algorithms can also be used for the MMV problem.

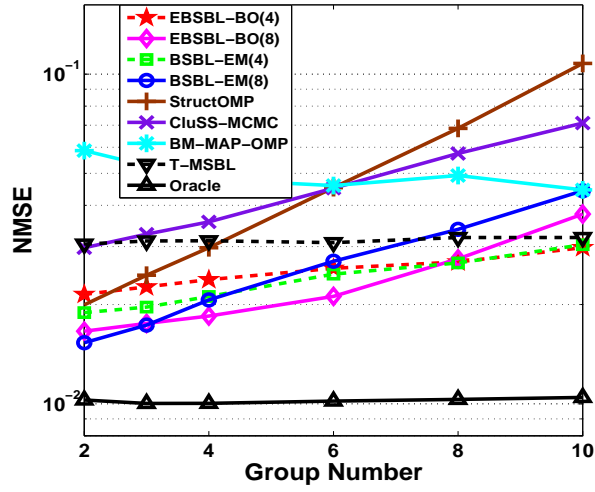


Fig. 6. Algorithms' performance when block partition was unknown.

The uniqueness of our algorithms is that they can explore and exploit intra-block correlation, which is widely present in practical applications. Our experiments showed that exploiting the intra-block correlation can greatly improve recovery performance. Based on our knowledge, it is the first time that intra-block correlation has been shown to be greatly helpful in improving algorithm performance for the block sparse model. By deriving a hybrid algorithm we show a promising approach to improve existing algorithms such that they can also exploit the correlation for better performance.

## REFERENCES

- [1] M. Yuan and Y. Lin, "Model selection and estimation in regression with grouped variables," *J. R. Statist. Soc. B*, vol. 68, pp. 49–67, 2006.
- [2] R. G. Baraniuk, V. Cevher, M. F. Duarte, and C. Hegde, "Model-based compressive sensing," *IEEE Trans. on Information Theory*, vol. 56, no. 4, pp. 1982–2001, 2010.
- [3] Y. C. Eldar, P. Kuppinger, and H. Bolcskei, "Block-sparse signals: uncertainty relations and efficient recovery," *IEEE Trans. on Signal Processing*, vol. 58, no. 6, pp. 3042–3054, 2010.
- [4] E. Van Den Berg and M. Friedlander, "Probing the pareto frontier for basis pursuit solutions," *SIAM Journal on Scientific Computing*, vol. 31, no. 2, pp. 890–912, 2008.
- [5] Y. C. Eldar and M. Mishali, "Robust recovery of signals from a structured union of subspaces," *IEEE Trans. on Information Theory*, vol. 55, no. 11, pp. 5302–5316, 2009.
- [6] J. Huang, T. Zhang, and D. Metaxas, "Learning with structured sparsity," in *Proceedings of the 26th Annual International Conference on Machine Learning*, 2009, pp. 417–424.
- [7] L. Yu, H. Sun, J. P. Barbot, and G. Zheng, "Bayesian compressive sensing for cluster structured sparse signals," *Signal Processing*, vol. 92, no. 1, pp. 259–269, 2012.

- [8] T. Faktor, Y. Eldar, and M. Elad, "Exploiting statistical dependencies in sparse representations for signal recovery," *Arxiv preprint arXiv:1010.5734*, 2010.
- [9] Z. Zhang and B. D. Rao, "Sparse signal recovery with temporally correlated source vectors using sparse bayesian learning," *IEEE Journal of Selected Topics in Signal Processing*, vol. 5, no. 5, pp. 912–926, 2011.
- [10] S. F. Cotter, B. D. Rao, K. Engan, and K. Kreutz-Delgado, "Sparse solutions to linear inverse problems with multiple measurement vectors," *IEEE Trans. on Signal Processing*, vol. 53, no. 7, pp. 2477–2488, 2005.
- [11] R. M. Neal, *Bayesian learning for neural networks*. Springer, 1996.
- [12] M. E. Tipping, "Sparse Bayesian learning and the relevance vector machine," *J. of Mach. Learn. Res.*, vol. 1, pp. 211–244, 2001.
- [13] D. J. C. MacKay, "Bayesian interpolation," *Neural Computation*, vol. 4, no. 3, pp. 415–447, 1992.
- [14] Z. Zhang and B. D. Rao, "Clarify some issues on the sparse bayesian learning for sparse signal recovery," *Technical Report, University of California, San Diego*, 2011.
- [15] M. Elad, *Sparse and redundant representations: from theory to applications in signal and image processing*. Springer Verlag, 2010.
- [16] E. J. Candes, M. B. Wakin, and S. P. Boyd, "Enhancing sparsity by reweighted  $\ell_1$  minimization," *J Fourier Anal Appl*, vol. 14, pp. 877–905, 2008.
- [17] P. Stoica and P. Babu, "SPICE and LIKES: Two hyperparameter-free methods for sparse-parameter estimation," *Signal Processing*, 2012.
- [18] Z. Zhang and B. D. Rao, "Exploiting correlation in sparse signal recovery problems: Multiple measurement vectors, block sparsity, and time-varying sparsity," in *ICML 2011 Workshop on Structured Sparsity: Learning and Inference*, 2011.
- [19] D. Wipf and S. Nagarajan, "Iterative reweighted  $\ell_1$  and  $\ell_2$  methods for finding sparse solutions," *IEEE Journal of Selected Topics in Signal Processing*, vol. 4, no. 2, pp. 317–329, 2010.
- [20] R. Tibshirani, J. Bien, J. Friedman, and et al, "Strong rules for discarding predictors in lasso-type problems," *J. R. Statist. Soc. B*, vol. 74, 2012.
- [21] Z. Xiang, Y. Xi, U. Hasson, and P. Ramadge, "Boosting with spatial regularization," in *Advances in Neural Information Processing Systems 22*, 2009, pp. 2107–2115.